桐柏杂岩北界剪切带的变质变形分析及归属讨论

李海龙,宋传中,李加好,任升莲,张妍,王微,杨帆
合肥工业大学资源与环境工程学院,合肥,230009

内容提要:秦岭—桐柏—大别碰撞造山带是世界上最大的高压—超高压构造带。通过对桐柏杂岩北界剪切带的观察分析得知,桐柏杂岩北界剪切带是一条左旋平移性质的韧性剪切带,该剪切带内多发育杆状构造,且杆状构造具有圈层结构,层与层之间通过一种特殊的滑脱面结合。经过镜下分析测量得知,桐柏杂岩北界剪切带的有限应变测量值 R_{xz} 在1.80~2.04之间,平均值为1.95,涡度值 W_k 在0.82~0.90之间,平均值为0.86,均大于0.75,说明桐柏杂岩北界剪切带是一条以简单剪切为主,纯剪切为辅的韧性剪切带,反映出此剪切带不是单纯的造山带挤压形成,还受到平行于造山带方向的剪切作用,可能与造山带碰撞后的折返机制有关。通过石英和长石的动态重结晶以及角闪石全Al压力计、角闪石—斜长石温度计和黑云母中Ti温度计可以得知桐柏杂岩北界剪切带的形成条件约为 $t=560$~684℃,$P=0.6$~0.9 GPa,属于高角闪岩相,处于中地壳流变层位置。通过与商丹断裂带(商南—丹凤断裂带)以及晓天—磨子潭剪切带的对比可以知道,桐柏杂岩北界剪切带可能对应晓天—磨子潭剪切带的西延部分,而不是商丹断裂带。

关键词:桐柏杂岩;韧性剪切带;圈层结构;滑脱面;有限应变;涡度

秦岭—桐柏—大别—苏鲁碰撞造山带(亦称中央造山带)是世界上最大的高压—超高压构造带,按照现今结构,从西向东可以将其分为五段:秦岭造山带、桐柏造山带、西大别造山带、东大别造山带和苏鲁造山带,也有学者将西大别造山带和东大别造山带合并成大别造山带。近几十年来,基于岩石学、同位素地球化学、构造地质学、地质年代学等相关资料,地质学家们提出了许多构造模式来解释该构造带的高压—超高压岩石的折返剥露机制,这些研究主要集中在大别—苏鲁造山带以及秦岭造山带,而对于中间的桐柏造山带以及西大别造山带研究较少(杨志坚, 1982; Okay et al., 1993; Webb et al., 1999; Hacker et al., 2000; Faure et al., 2003; Zheng Yongfei et al., 2003, 2007; Xu et al., 2006; 徐备等, 2007; Zhou et al., 2008; Liu Xiaochun et al., 2008a; Wu Yuanbao et al., 2008; 刘鑫等, 2010; 刘晓春等, 2011)。桐柏碰撞造山带是秦岭造山带与大别—苏鲁造山带的连接纽带,是华北地块与扬子地块,及其之间所夹持的南秦岭微陆块于中生代碰撞拼合的产物(张国伟等, 1996; Li et al., 2007)。桐柏碰撞造山带主体由两部分组成:桐柏核部杂岩和两侧的高压岩片单元(刘鑫等, 2010)。

关于桐柏造山带的构造格局前人有不同的看法,其中桐柏山背形构造已经被多数地质学家认同(王国灿, 1996; 黄少英, 2006; 许光等, 2010; 刘晓春, 2011, 2013)。桐柏造山带背形构造核部为一套桐柏杂岩,其岩性以片麻状花岗岩为主,两侧对称发育两条榴辉岩带,构成背形构造的两翼(崔建军, 2009; 刘晓春等, 2013),桐柏杂岩与两条榴辉岩带之间则发育两条大型的韧性剪切带,而关于桐柏杂岩和南北两条韧性剪切带之间的关系尚不明确(刘欢等, 2014)。近期笔者在桐柏杂岩中发现有大型杆状构造、糜棱岩、以及L构造岩和圈层结构等重要的构造现象,这些现象集中出现在桐柏杂岩北界312国道附近,为研究桐柏杂岩北界剪切带的韧性变形提供了重要标志,同时对于认识桐柏杂岩与北侧韧性剪切带的构造关系以及桐柏山的构造发展演化具有重要的地质意义。

1 地质概况

桐柏造山带位于秦岭—桐柏—大别—苏鲁造山带的中部,是连接秦岭造山带与大别—苏鲁造山带

注:本文为国家自然科学基金资助项目(编号:41272222、41502193)的成果。
投稿日期:2016-09-06;改回日期:2017-02-17;责任编辑:刘志强。Doi: 10.16509/j.georeview.2017.02.008
作者简介:李海龙,男,1991年生。博士研究生,构造地质学专业。Email:sargnlee@126.com。通讯作者:宋传中,男,1954年生。教授,博士生导师,构造地质学专业。Email:czsong69@163.com。

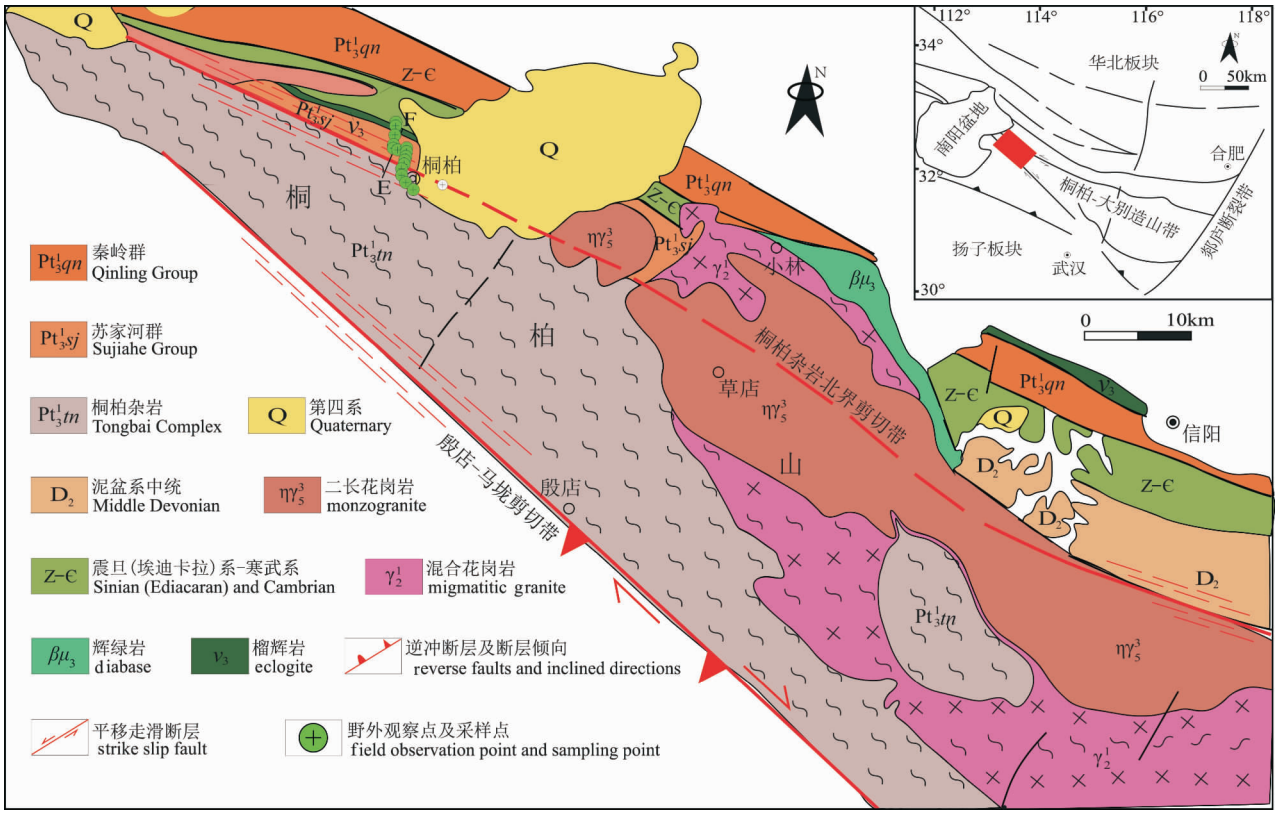


图 1 桐柏造山带地质简图

Fig. 1 The geological sketch map of the Tongbai orogenic belt

的纽带,构造挤出作用导致桐柏造山带在地表形貌上是西窄东宽,类似一个楔形地体(图 1)。向西越过南阳盆地与秦岭造山带相连,向东以大悟断裂为界与大别—苏鲁造山带相接(张宏飞等,1999;董云鹏等,2003;张本仁等,2005;Liu Xiaochun et al.,2005;徐备等,2007;刘鑫等,2010;刘晓春等,2011)。刘鑫等人(2010)通过野外构造解析,依据新的地质年代学资料,将桐柏造山带及其邻区划分为 9 个岩石构造单元,由北向南依次是:华北克拉通南缘岩石构造单元、二郎坪岩石构造单元、秦岭杂岩、龟山岩组和南湾岩组、构造混杂岩带、桐柏北部高压片岩、桐柏核部杂岩单元、桐柏南部高压岩片以及随州构造变形带。Liu Xiaochun 等(2005,2008,2011,2013)认为桐柏造山带主要由两套造山系统构成,北侧为古生代增生造山系统,南侧为中生代碰撞造山系统。其中古生代增生造山系统包括宽坪群、二郎坪群、秦岭群、龟山杂岩和南湾复理石。中生代碰撞造山系统则包括八里畈构造混杂岩带(定远组)、北部榴辉岩带(浒湾组)和桐柏杂岩、南部榴辉岩带和蓝片岩—绿片岩带。这些岩石构造单元构成了桐柏山背形的核部和两翼,基本上可以与西大别高压—超高压变质地体相对比,其中最重要的差别在于核部桐柏杂岩的产出以及超高压变质单元的缺失,对于超高压单元的缺失,绝大多数研究者推测,这种变质条件的规律性变化缘于造山带向西抬升幅度逐渐变小,致使超高压岩石在秦岭—桐柏地区未能出露于地表(Zhang et al.,1994;Zhang et al.,2004;Ernst et al.,2007)。刘晓春等(2011)认为桐柏地区超高压岩石的缺乏可能缘于华南陆块的俯冲深度向西变浅,大陆深俯冲作用只局限于大别—苏鲁地区。实际上,桐柏杂岩的出露说明桐柏地区的抬升幅度至少不低于西大别地区。

详细的构造解析和年代学资料表明桐柏—大别—苏鲁造山带的最终构造框架定格于早白垩世的构造伸展事件(Eide et al.,1994;Hacker et al.,1995,2000;Webb et al.,1999,2001;Faure et al.,1999,2003;Ratschbacher et al.,2000;索书田等,2001a,b;Wang et al.,2003;Lin Wei et al.,2009;Li Sanzhong et al.,2009,2010)。这一构造事件导致了桐柏—大别高压—超高压变质地体向东的侧向挤

出。

2　桐柏杂岩北界剪切带的变形分析

李炳华等(2001)的区域重磁场特征研究认为:丹凤—商南—西峡—桐柏—商城—庐江大剪切带是秦岭主造山期板块的俯冲碰撞缝合带,总体呈北西向展布,中部为近东西向,自新元古代末起就是扬子板块与华北板块的边界。商丹断裂带作为两大板块的缝合线已经被多数地质学家认可(张国伟等,1998,2001;钟增球等,2001;宋传中,2000;宋传中等,2009)。桐柏杂岩北界剪切带在桐柏山地区以桐柏杂岩北界断裂形式出现。

地质学者研究较多的是秦岭造山带里的一些剪切带(李加好等,2010;任升莲等,2011;涂文传等,2012),而对于桐柏杂岩北界剪切带研究的较少。这里所说的桐柏杂岩北界剪切带是指桐柏杂岩北部的一个剪切带,由于此剪切带位于华北板块与扬子板块碰撞缝合线附近,所以岩石单元以及构造现象比较复杂,导致了剪切带弯曲的现象。

2.1　运动学分析

桐柏杂岩北界剪切带在桐柏杂岩北界主要岩性出露有初糜棱岩、糜棱岩、超糜棱岩、混合岩、片麻岩、片岩等。通过对野外片麻岩以及糜棱岩中构造现象的分析可以知道,桐柏杂岩北界剪切带是一条左旋平移的大型韧性剪切带。这些构造现象包括糜棱岩中不对称钾长石残斑(图 2d、图 3e、3f),小型韧性剪切(图 2b、2h),白云片岩中的 S－C 组构(图 2e)以及混合岩透镜体(图 2f)等,这些构造标志说明桐柏杂岩北界剪切带是左行走滑剪切的。

从图 2 的剖面图可以看出,商丹剪切带东延段的产状整体上倾向北北东—北东方向,与桐柏山南缘的殷店—马垅剪切带的产状(韩建军等,2014)是相背的,这也印证了桐柏山的背形构造,而商丹剪切带东延段则构成了桐柏山背形构造的北翼。从剖面北端到剖面南端,岩性是发生变化的,经历片麻岩→片岩→混合岩→糜棱岩→超糜棱岩→糜棱岩→初糜棱岩→混合岩→片麻岩的转变过程,从岩性变化可以看出来,剪切带内的变形强度从北到南,由弱变形带→强变形带→弱变形带的变化,在大水磨湾处出露大量的超糜棱岩,对应着变形最强烈的位置。

从图 3a、b、d 可以看出,桐柏杂岩北界剪切带中多见杆状构造,且杆状构造之间具有分层结构,层与层之间通过一种特殊的物质连接,这种物质类似滑脱面(图 3c),并且这种特殊物质的表面保留着热擦痕,这种擦痕应该是剪切带活动导致层与层之间发生滑动而产生的,通过热擦痕的方向也能判断出运动方向为左旋平移。

2.2　有限应变测量及涡度分析

为了查明该地区由于韧性剪切变形而造成的岩石有限应变特征及规律,本次从剪切带内选择 11 块标本进行岩石的有限应变测量。样品编号分别是 XY-25、XY-27、XY29-1、XY29-2、XY-30、XY-31、XY32-1、XY-33、XY-35、XY-36、XY-37。有限应变测量采用长短轴法,显微镜下对 XZ 面上的变形长石进行测量统计(至少 50 组),计算其长短轴比。

自然界中的剪切变形通常具有纯剪切变形和简单剪切变形两个端元,通过常规方法很难获得纯剪切和简单剪切在剪切变形中相对大小的信息,而涡度分析则有助于解决此问题。涡度(W_k)的概念来源于流体力学,是某一运动形式所拥有的旋转量,在地质学中主要应用于应变非共轴程度的确定。在剪切变形中,完全为纯剪切变形时,$W_k=0$;完全为简单剪切变形时,$W_k=1$。在一般剪切中,W_k值介于 0 和 1 之间。但是 $W_k=0.5$ 时并不意味着纯剪切与简单剪切各占一半,只有在 $W_k=0.75$ 时才表示纯剪切与简单剪切的作用相等,这种现象称为“纯剪倾向性”(Tikoff et al.,1995;郑亚东等,2008;李加好等,2010)。根据郑亚东等(2008)得知有限应变与涡度之间的关系,通过这个关系可以测得涡度(W_k)值,关系表达式为:

$$W_k=\sin\left[\arctan\left(\frac{\sin 2\theta}{\frac{R_{xz}+1}{R_{xz}-1}}-\cos 2\theta\right)\right]\cdot\frac{R_{xz}+1}{R_{xz}-1} \tag{1}$$

关系式(1)中的 θ 为钾长石长轴方向与剪切方向的锐夹角,R_{xz}为有限应变,即长轴与短轴的比值。从关系式可以看出来,只要测得钾长石的长短轴之比 R_{xz}以及长轴与剪切方向的锐夹角 θ,既可以得知涡度值,测量的结果见表 1。

从表 1 可以看出来,桐柏杂岩北界剪切带中岩石的有限应变 $R_{xz}=1.80\sim2.04$,平均值为 1.95,并且从剪切带北侧到南侧,R_{xz}发生微弱的变化,总体上从北到南先变强再变弱,差异比较小。而涡度的取值范围为 $W_k=0.82\sim0.90$,平均值为 0.86,均大于 0.75,由此可以知道,桐柏杂岩北界剪切带是一条以简单剪切为主,纯剪切为辅的韧性剪切带。这反映出此剪切带不是单纯的造山带挤压形成,还受

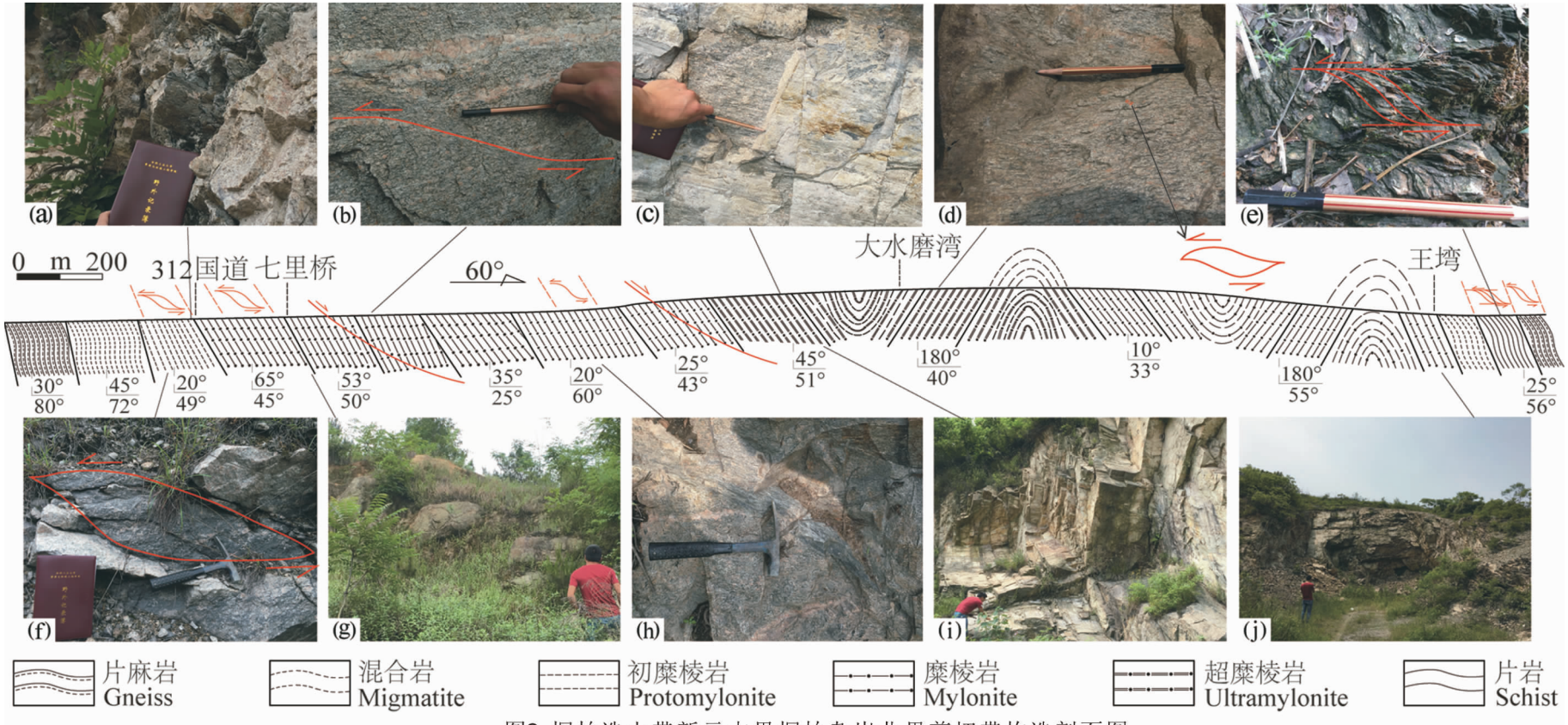


图2 桐柏造山带新元古界桐柏杂岩北界剪切带构造剖面图

Fig. 2 The structural profile of the shear zone in northern boundary of the Neoproterozoic Tongbai Complex in the Tongbai orogenic belt

(a)—312国道旁糜棱岩中的杆状构造；(b)—312国道旁糜棱岩中小型的韧性剪切；(c)—层与层之间的滑脱面；(d)—糜棱岩中的钾长石残斑；(e)—白云片岩中的S-C组构；(f)—312国道旁混合岩透镜体；(g)—312国道旁糜棱岩中的杆状构造；(h)—312国道旁糜棱岩中小型的韧性剪切；(i)—大水磨湾糜棱岩的分层；(j)—王垮大型杆状构造

(a)—Rod structure in the mylonite beside 312 National Road；(b)—Small ductile shear in the mylonite beside 312 National Road；(c)—Detachment surface between layers；(d)—K-feldspar porphyroclast in the mylonite；(e)—S-C fabric in Muscovite schist；(f)—The migmatite lens beside 312 National Road；(g)—Rod structure in the mylonite beside 312 National Road；(h)—Small ductile shear in the mylonite beside 312 National Road；(i)—The layer structure in the mylonite in Dashuimo Bay；(j)—Large rod structure in the mylonite in Wangwan

到平行于造山带方向的剪切作用,可能与造山带碰撞后的折返机制有关系。此处的剪切带与大别山北侧的晓天—磨子潭断裂相似,王勇生等(2008)对晓天—磨子潭进行了涡度分析,其涡度值均大于 0.9,也是属于简单剪切变形,指示了造山带在折返至中—下地壳过程中的折返驱动力为浮力。

3　桐柏杂岩北界剪切带的变质环境分析

构造变形环境的确定是构造成因分析的一个重要内容,同时也是厘定构造层次的重要依据。而温压条件很大程度上限制了矿物的变形机制、变形方式以及不同岩石的变形类型。

笔者先根据岩石中石英和长石矿物的动态重结晶样式来半定量来估算温度,然后再利用角闪石—斜长石—石英温度计以及角闪石全 Al 压力计,结合黑云母 Ti 温度计等地质温度计来定量计算其温压条件。

3.1　变质温度的半定量分析

向必伟等(2007)和 Daalen 等(1999)的研究表明,石英在 250℃以下为脆性破裂;250 ~ 300℃时呈现为波状消光、塑性变形,并伴有颗粒边缘亚颗粒化;300 ~ 380℃时残斑颗粒间出现膨凸式重结晶(BLG)以及颗粒边缘亚颗粒化;380 ~ 420℃范围内由膨凸式重结晶(BLG)向亚颗粒旋转式重结晶(SR)转变,两种重结晶形式共存,约 420℃时转变结束;420 ~ 480℃以独立的亚颗粒旋转式重结晶(SR)存在;480 ~ 530℃区间重结晶由亚颗粒旋转式重结晶(SR)向颗粒边界迁移式重结晶(GBM)转变,两种颗粒边界形式共存;530 ~ 630℃时呈独立的颗粒边界迁移式重结晶(GBM)形式。

表 1 桐柏造山带新元古界桐柏杂岩北界剪切带中岩石有限应变测量及涡度值

Table 1 The finite strain and vorticity value in the shear zone in northern boundary of the Neoproterozoic Tongbai Complex in the Tongbai orogenic belt

样品	岩性	测量组数	有限应变 R_{xz}	涡度 W_k
XY-25	长英质片麻岩	56	1.80	0.82
XY-27	白云斜长片麻岩	54	1.88	0.83
XY29-1	长英质糜棱岩	52	1.92	0.86
XY29-2	长英质超糜棱岩	55	1.94	0.84
XY-30	长英质超糜棱岩	57	1.97	0.86
XY-31	长英质超糜棱岩	51	2.01	0.90
XY32-1	长英质超糜棱岩	50	2.04	0.87
XY-33	长英质超糜棱岩	55	2.03	0.86
XY-35	长英质糜棱岩	52	1.99	0.85
XY-36	长英质糜棱岩	53	1.96	0.87
XY-37	长英质糜棱岩	56	1.91	0.88
平均值	—	—	1.95	0.86

长石的变形机制与温度的相关性也有类似石英的规律。长石在低于 300℃完全为脆性破裂;在 300 ~400℃时以显微破裂、波状消光、双晶纹弯曲为特征(Pryer et al. ,1993);400 ~ 500℃呈现塑性拉长以及颗粒边缘亚颗粒化(Simpson,1985;Cates,1989);长石重结晶从约 500℃开始,在 500 ~ 650℃温度范围内表现为 BLG 重结晶,可见颗粒边界的不规则突入和镶嵌构造;650 ~ 700℃时由 BLG 向 SR 转变,两类重结晶型式共存;700 ~ 800℃温度区间内呈现独立的 SR 重结晶(Lafrance et al. ,1998);800 ~ 850℃为长石的 SR 重结晶向 GBM 重结晶转变的范围,两种重结晶形式共存;850℃以上时长石呈现独立的 GBM 重结晶(Anderson et al. ,1993)。

桐柏杂岩北界剪切带出露的岩石类型丰富,有片麻岩、混合岩、初糜棱岩、糜棱岩、超糜棱岩等,其中长石和石英的变形较为丰富,镜下清晰可见,为估算变形温度提供了便利条件。此次在桐柏杂岩北界剪切带剖面上,从北到南选取了 10 块具有代表性的标本进行镜下观察分析,观察结果见图 4。根据长石、石英的变形机制,对相应的变形温度做了半定量估算。结果见表 2。

根据石英以及长石的动态重结晶形态(表 2)可以看出,桐柏杂岩北界剪切带的变形温度范围大约在 560 ~ 660℃的区间。

3.2　变质条件的定量分析

桐柏杂岩北界剪切带的岩性主要为糜棱岩化的片麻岩、初糜棱岩、糜棱岩以及超糜棱岩。为了探讨桐柏杂岩北界剪切带的形成温度和形成压力,此次分析选取了 6 块剪切带上岩石进行电子探针分析实验,并对其进行了相关的温度、压力计算。电子探针片由合肥工业大学磨片室完成,矿物成分分析由合肥工业大学电子探针实验室完成,仪器型号为:JXA-8230;实验条件为:加速电压 15kV,电子束流 20nA,电子束斑直径 3μm。

样品编号分别是 XY-30、XY-31、XY-33、XY-35、XY-37 和 XY-39。其中 XY-30、XY-31、XY-33、XY-35 和 XY-37 属于长英质超糜棱岩和长英质糜棱岩,均采自剪切带上;XY-39 是糜棱岩化的片麻岩,采自剪切带上,主要矿物组合为石英 + 斜长石 + 角闪石 + 钾长石 + 黑云母,呈细密条带状,浅色矿物和深色矿

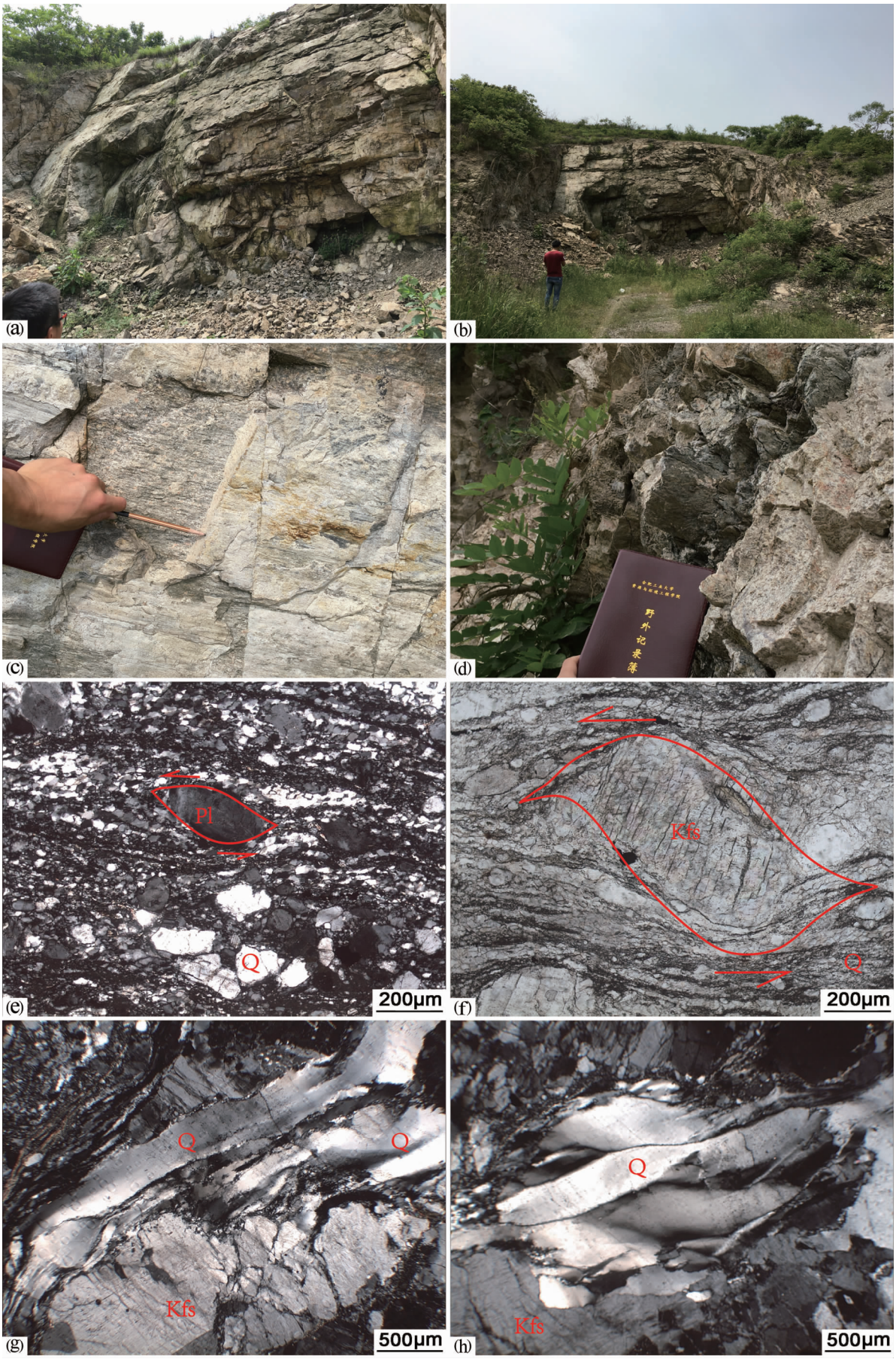

(a)
(b)
(c)
(d)
野外记录簿
(e)
Pl
Q
200μm
(f)
Kfs
Q
200μm
(g)
Q
Q
Kfs
500μm
(h)
Q
Kfs
500μm

图 3 桐柏造山带新元古界桐柏杂岩北界剪切带野外照片及镜下显微照片

Fig. 3 The field photographs and micrographs of the shear zone in northern boundary of the Neoproterozoic Tongbai Complex in the Tongbai orogenic belt

(a)、(b)—剪切带北端巨型杆状构造以及分层结构;(c)—杆状构造中层与层之间的特殊物质(滑脱面)以及热擦痕;(d)—糜棱岩中的杆状构造;(e)、(f)—镜下钾长石的不对称残斑以及糜棱岩的流动构造;(g)、(h)—糜棱岩中石英的单晶条带以及拔丝构造。Kfs—钾长石;Q—石英;Pl—斜长石

(a),(b)—Large rod structure and layer structure in northern tip of the shear zone;(c)—Detachment surface between layers and heated scratch in the rod structure;(d)—Rod structure in the mylonite;(e),(f)—K-feldspar porphyroclast under the microscope and flow structure of the mylonite;(g),(h)—Single crystal band and wire drawing structure of quartz in the mylonite

物相间排列,透入性片麻理发育,并且产状与剪切带糜棱岩的产状一致(图 2)。根据这些特征判断该片麻岩属于强直片麻岩。

强直片麻岩是高级变质区发育的一种细密条带状或条纹状构造片麻岩。岩石中矿物分带性明显,或由浅色矿物和暗色矿物相间排列组成间隔较密而平直的条带或条纹。有时可见拉伸线理,形成 SL 组构。强直片麻岩是在中、深变质环境强应变带(韧性剪切流变带)中形成的,有明显的剪切流变特征,其空间分布常呈一定宽度的带状。由此判断该片麻岩(XY-39)与邻区的韧性剪切带内糜棱岩应属于同期构造产物。

由于长英质糜棱岩以及长英质超糜棱岩中没有合适的矿物组合来直接计算温压条件,所以可以通过研究糜棱岩化强直片麻岩的形成环境来反映剪切带的形成条件,因为强直片麻岩是在中、深变质环境强应变带(韧性剪切流变带)中形成的。经过镜下分析可见,强直片麻岩中角闪石和斜长石共生,因此可利用角闪石全铝压力计来计算形成压力,用角闪石—斜长石温度计来计算形成温度。为了保证准确度以及可信度,同时利用黑云母 Ti 温度计加以辅佐验证,在长英质糜棱岩以及长英质超糜棱岩基质中含有黑云母条带,是伴随着剪切带形成的,所以通过基质中的黑云母计算出的温度可以反映出剪切带形成的条件。

根据强直片麻岩中角闪石和斜长石的探针结果,依次采用 Hammarstrom 等(1986)、Hollister 等(1987)、Johnson 等(1988,1989)、Schmidt(1992)、汪洋(2014)建立的角闪石全铝地质压力计公式进行计算,得到角闪石的形成压力,结果见表 3。再根据 Holland 和 Blundy 等(1994)建立的角闪石—斜长石—石英地质温度计来计算出角闪石和斜长石的形成温度,计算结果见表 4。

从角闪石—斜长石—石英地质温度计以及角闪石全铝压力计的计算结果可以看出,强直片麻岩的形成压力为 0.6 ~ 0.9 GPa,形成温度约为 587 ~ 684℃,平均温度为 632℃,属于高角闪岩相变质范畴,此结果与通过石英、长石的动态重结晶半定量得出来的结果是近乎一致的。为了验证这一结果能否反映出整个剪切带的形成条件,利用剪切带中糜棱岩、超糜棱岩中基质黑云母进行探针测试。然后再根据吴春明等(2015)提出的黑云母中的 Ti 来计算变质温度,公式表达为:

$$\ln(t/℃) = 6.313 + 0.224\ln w(\mathrm{Ti}) - 0.228\ln w(\mathrm{Fe}) - 0.449\ln w(\mathrm{Mg}) + 0.15(P/\mathrm{GPa}) \quad (2)$$

公式(2)中的 $w(\mathrm{Ti})$、$w(\mathrm{Fe})$、$w(\mathrm{Mg})$ 是通过对黑云母的探针数据利用 Minpet2.02 软件计算得到的阳离子数。该公式适用条件为变质温度在 450 ~ 840℃,压力在 0.1 ~ 1.9GPa。该公式适合于自然界

表 2 桐柏造山带新元古界桐柏杂岩北界剪切带内岩石显微鉴定及温度估算

Table 2 Microscopic identification and temperature estimation in the shear zone in northern boundary of the Neoproterozoic Tongbai Complex in the Tongbai orogenic belt

样品	岩石类型	矿物组合	动态重结晶类型		估算变形温度(℃)
			石英	斜长石	
XY-25	长英质片麻岩	Q + Pl + Kfs + Ms + Bt	GBM	BLG	560
XY29-1	长英质糜棱岩	Q + Pl + Kfs	GBM	BLG	580
XY29-2	长英质超糜棱岩	Q + Pl + Kfs + Ms	GBM	BLG→SR	650
XY-30	长英质超糜棱岩	Q + Pl + Kfs + Ms + Bt	GBM	BLG→SR	660
XY-31	长英质超糜棱岩	Q + Pl + Kfs + Bt	GBM	BLG→SR	650
XY32-1	长英质超糜棱岩	Q + Pl + Kfs + Ms + Bt	GBM	BLG→SR	660
XY-33	长英质超糜棱岩	Q + Pl + Kfs + Ms + Bt	GBM	BLG→SR	660
XY-35	长英质糜棱岩	Q + Pl + Kfs + Ms + Bt	GBM	BLG	600
XY-36	长英质糜棱岩	Q + Pl + Kfs + Ms + Bt	GBM	BLG	620
XY-37	长英质糜棱岩	Q + Pl + Kfs + Ms + Bt	GBM	BLG	620

注:Q—石英;Ms—白云母;Bt—黑云母;Pl—斜长石;Kfs—钾长石。

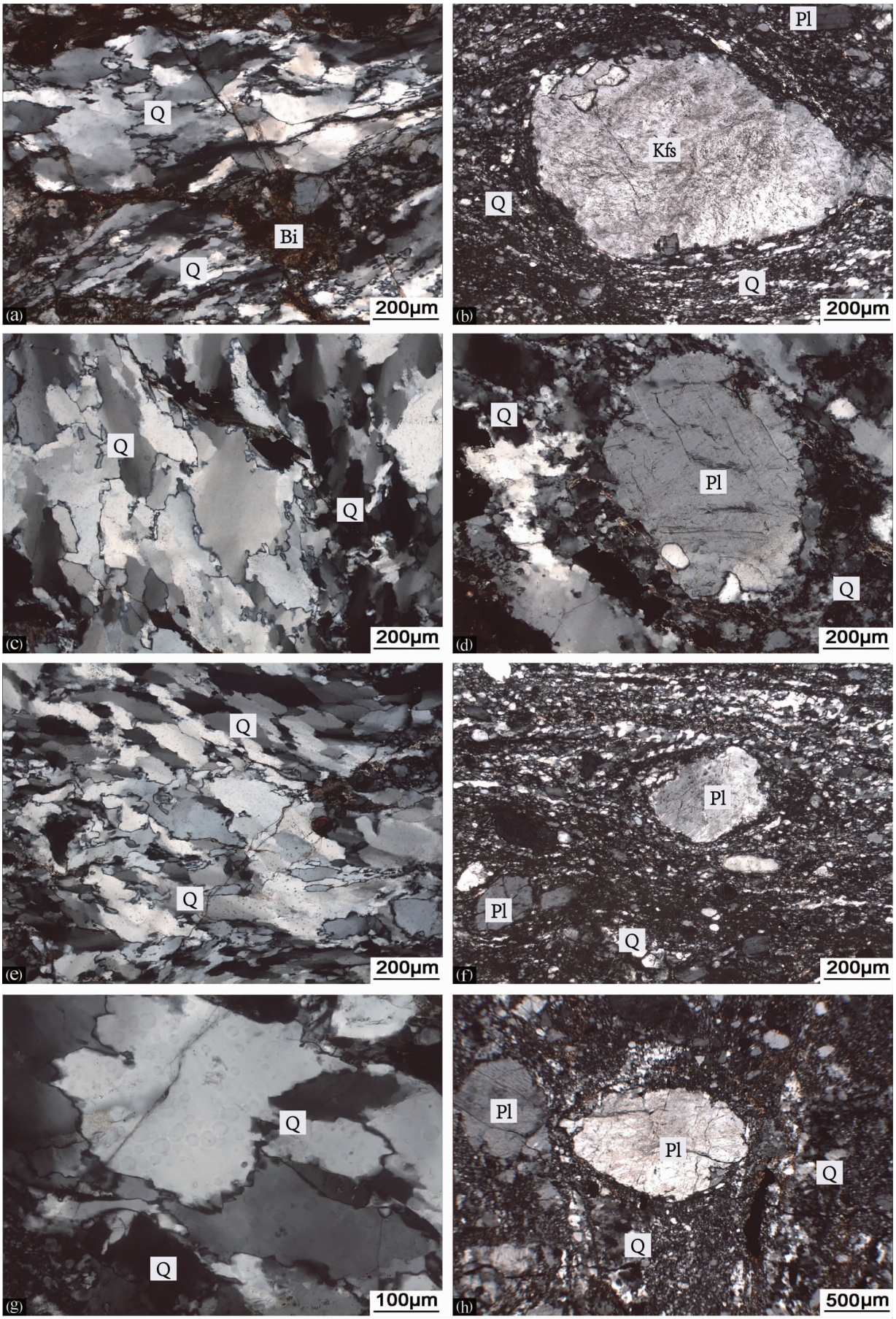

Q
Bi
Q
200μm
(a)
Pl
Kfs
Q
Q
200μm
(b)
Q
Q
200μm
(c)
Q
Pl
Q
200μm
(d)
Q
Q
200μm
(e)
Pl
Pl
Q
200μm
(f)
Q
Q
100μm
(g)
Pl
Pl
Q
Q
500μm
(h)

图 4 桐柏造山带新元古界桐柏杂岩北界剪切带矿物的动态重结晶

Fig. 4 The mineral dynamic recrystallization in the shear zone in northern boundary of the Neoproterozoic Tongbai Complex in the Tongbai orogenic belt

(a)、(c)、(e)、(g)—石英的边界迁移式式动态重结晶;(b)、(d)、(f)、(h)—长石的核幔构造及膨凸式动态重结晶

(a),(c),(e),(g)—Boundary migration dynamic recrystallization of the quartz;(b),(d),(f),(h)—Core—mantle fabric and bulge type dynamic recrystallization of the feldspar

98%以上的黑云母,误差为 ±50℃。从公式(2)可以看出,压力的单位为 GPa,并且系数为 0.15,因此在计算温度时,压力的影响是非常小的,可以忽略不计。

表 3 桐柏造山带新元古界桐柏杂岩北界剪切带强直片麻岩中角闪石全铝压力计所计算的变质压力(单位:GPa)

Table 3 The metamorphic pressure of hornblende total Al pressure gauge in the straight gneiss of the shear zone in north boundary of the Neoproterozoic Tongbai Complex in the Tongbai orogenic belt (Unit:GPa)

样品	P1	P2	P3	P4	P5	P6
XY-39-1	0.76	0.82	0.63	0.62	0.79	0.76
XY-39-2	0.76	0.81	0.62	0.62	0.79	0.76
XY-39-3	0.80	0.86	0.66	0.66	0.83	0.80
XY-39-4	0.80	0.86	0.66	0.65	0.82	0.80
XY-39-5	0.83	0.89	0.68	0.68	0.85	0.83
XY-39-6	0.82	0.88	0.67	0.67	0.84	0.82
XY-39-7	0.74	0.79	0.61	0.61	0.77	0.74
XY-39-8	0.74	0.80	0.61	0.61	0.77	0.75
XY-39-9	0.74	0.79	0.61	0.61	0.77	0.74
XY-39-10	0.80	0.86	0.66	0.66	0.83	0.80
XY-39-11	0.80	0.86	0.66	0.65	0.82	0.80
XY-39-12	0.79	0.85	0.65	0.65	0.82	0.79
XY-39-13	0.77	0.83	0.63	0.63	0.80	0.77
XY-39-14	0.80	0.86	0.66	0.66	0.83	0.81
XY-39-15	0.81	0.87	0.67	0.66	0.84	0.81
平均压力	0.78	0.84	0.65	0.64	0.81	0.79

注:P_1、P_2、P_3、P_4、P_5、P_6 分别为 Hammarstrom 等(1986)、Hollister 等(1987)、Johnson 等(1988,1989)、Schmidt(1992)、Anderson 等(1995)、汪洋(2014)公式计算所得压力。

根据黑云母中 Ti 温度计的计算结果(表 5)可以知道,桐柏杂岩北界剪切带的形成温度约为 560~680℃,平均温度 622℃。通过黑云母 Ti 温度计计算的温度与角闪石—斜长石—石英温度计计算的结果几乎一致,因此可以说明强直片麻岩是在韧性剪切流变带中形成的,即强直片麻岩形成环境与剪切带的形成环境是吻合的。所以可以认为,桐柏杂岩北界剪切带的形成条件压力为 $P=0.6\sim0.9$GPa,形成温度约为 $t=560\sim684$℃,属于高角闪岩相变质范畴,形成深度约 25km 左右,处于中地壳流变层。

4　桐柏杂岩北界剪切带的归属讨论

秦岭—桐柏—大别—苏鲁造山带又被称为中央造山带,是中国南北划分的界线,是一条横贯中国东西部的大型造山带,是由于印支期华北板块与华南板块碰撞形成的。在两大板块碰撞之前,之间是被原特提斯洋隔开的,原特提斯洋是从新元古代 Rodinia 裂解到早古生代发育于滇缅泰/保山微陆块以北、塔里木—华北陆块以南的一个复杂成因的洋盆。长期以来对原特提斯洋的南、北边界及其早古生代末俯冲极性还存在争论。李三忠等(2016a)利用野外地质、构造、岩浆、沉积学、地球化学、构造年代学和层析成像等最新成果,以期界定原特提斯域的南、北边界位置,确定原特提斯洋边界俯冲极性。集成分析结果表明,北界为古洛南—栾川缝合线(或宽坪缝合线)及其直至西昆仑的西延部分;南界为龙木措—双湖—昌宁—孟连缝合线。李三忠等(2016b)认为早古生代早期除华北陆块不具有亲冈瓦纳大陆的特征外,扬子、华夏、塔里木、柴达木、阿拉善、北秦岭—中祁连—中阿尔金、欧龙布鲁克、北羌塘、南羌塘、拉萨、兰坪-思茅、印支等陆块/微陆块都具有亲冈瓦纳的特征。在 450~400Ma 左右这一系列陆块/微陆块都向南俯冲—增生,并逐步拼合于冈瓦纳大陆北缘东段,原特提斯洋关闭,并形成了原潘吉亚(Proto-Pangea)超大陆;原潘吉亚于 380Ma 以后裂离出塔里木—华北陆块和大华南陆块,分别出现勉(县)略(阳)洋和古特提斯洋,直到 240~220Ma 逐步向北聚合,形成最终的劳亚古陆,此时才形成潘吉亚超大陆。

随着勉略洋和古特提斯洋的闭合,华北板块与扬子板块碰撞分别形成了勉略带和商单带,所以勉(县)略(阳)带和商丹带是碰撞早期就形成的。由于板块的持续挤压碰撞,在缝合带附近又形成了一系列次级剪切带,而且这些次级剪切带是成对出现的,两两剪切带控制中间的夹块东西向运动。北秦岭造山带位于华北陆块与南秦岭微陆块的衔接部

位,是研究原特提斯洋构造演化的关键区域之一。北秦岭造山带内主要发育四条韧性剪切带,包括位于边界处的洛南—栾川剪切带和商丹剪切带,及其内部的官坡—乔端剪切带和朱阳关—夏馆剪切带(赵淑娟等,2016)。通过早期的构造演化可以知道,商丹带是板块碰撞早期就形成的,随后由于持续的挤压碰撞导致一些微陆块东西运动,与此同时伴随着一些次级剪切带的形成。而本文研究的桐柏杂岩北界剪切带应该就是商丹带伴生的次级剪切带,所以从这个角度来讲,桐柏杂岩北界剪切带与商单断裂带是不同时期不同体制下的产物。为了对桐柏杂岩北界剪切带的属性进一步了解,笔者根据晚期剥露的产物来进行综合对比分析。

关于桐柏杂岩北界剪切带,不少地质学者也做了不少研究,有学者认为该剪切带是商丹断裂带的东延部分(游振东等,1999;任升莲等,2011),并将其称作桐商(桐柏—商城)断裂带。还有学者认为该剪切带应属于晓天—磨子潭剪切带(刘欢等,2016)。本文将通过桐柏杂岩北界剪切带和商丹断裂带以及晓天—磨子潭剪切带的对比来探究其归属问题。

(1)桐柏杂岩北界剪切带是一条左旋平移剪切的韧性剪切带,商丹断裂带和晓天—磨子潭也是左旋平移的剪切带(宋传中等,2009;黄鹏等,2015;向必伟等,2007)。所以通过运动学方向不足以判定。

(2)经过测量,桐柏杂岩北界剪切带的有限应变为 $R_{xz}=1.80\sim2.04$,平均值为 1.96;涡度为 $W_k=0.82\sim0.90$,平均值为 0.86,均大于 0.75,属于以简单剪切为主的变形。宋传中等(2009)在商丹断裂带研究中得出的有限应变 $R_{xz}=4.21$;李加好等(2011)在商丹断裂带研究中得出的涡度值为 $W_k=0.54\sim0.67$,均小于 0.75,故得知商丹断裂带是以纯剪切为主的一般剪切。王勇生等(2008)在晓天—磨子潭剪切带研究中得到涡度值为 $W_k=0.913\sim0.995$,均大于 0.75,指示晓天—磨子潭剪切带的变形是简单剪切为主的变形。从这个角度来看,桐

表 4 桐柏造山带新元古界桐柏杂岩北界剪切带中强直片麻岩中角闪石和斜长石的探针数据以及角闪石—斜长石温度计计算结果

Table 4 The probe data of hornblende and plagioclase and the result of hornblende—plagioclase thermometer in the straight gneiss of the shear zone in northern boundary of the Neoproterozoic Tongbai Complex in the Tongbai orogenic belt

样品(XY)	39-1	39-2	39-3	39-4	39-5	39-6	39-7	39-8	39-9	39-10	39-11	39-12	39-13	39-14	39-15
t(℃)	587	684	624	639	623	641	641	616	653	620	643	609	641	622	641
角闪石															
SiO_2	43.83	43.29	43.01	42.86	42.73	42.72	43.76	43.83	43.32	43.11	42.86	43.32	43.48	43.25	42.93
TiO_2	0.39	0.34	0.30	0.34	0.24	0.32	0.38	0.43	0.35	0.19	0.36	0.34	0.28	0.32	0.30
Al_2O_3	12.90	12.90	13.21	13.19	13.55	13.42	12.68	12.69	12.57	13.29	13.21	13.20	12.98	13.34	13.38
FeO	17.09	19.31	17.76	17.40	17.44	17.36	17.24	17.24	17.62	17.74	17.26	17.46	17.68	17.64	17.50
MgO	9.20	9.44	9.16	9.49	9.24	9.43	9.77	9.45	9.52	9.12	9.18	9.04	9.54	9.20	9.36
CaO	11.13	10.61	10.68	10.90	11.26	10.92	10.99	10.93	11.06	11.24	11.68	11.21	10.89	10.93	11.23
Na_2O	1.49	1.57	1.41	1.55	1.41	1.47	1.41	1.41	1.42	1.47	1.26	1.41	1.43	1.48	1.38
K_2O	0.09	0.02	0.05	0.05	0.07	0.08	0.06	0.07	0.03	0.07	0.06	0.07	0.06	0.05	0.07
总量	96.12	97.48	95.58	95.78	95.94	95.72	96.29	96.05	95.89	96.23	95.87	96.05	96.34	96.21	96.15
斜长石															
SiO_2	62.00	61.87	61.53	61.36	62.02	62.04	60.03	61.51	61.61	61.89	60.76	61.23	60.84	60.61	60.85
TiO_2	0.00	0.00	0.03	0.00	0.00	0.05	0.00	0.00	0.00	0.00	0.03	0.00	0.05	0.00	0.00
Al_2O_3	24.19	24.22	24.25	24.08	23.64	24.19	23.46	24.22	24.18	24.07	24.47	24.35	24.34	24.88	24.24
FeO	0.08	0.13	0.13	0.18	0.23	0.12	0.07	0.04	0.04	0.08	0.05	0.09	0.08	0.13	0.08
MnO	0.06	0.00	0.01	0.09	0.00	0.05	0.00	0.00	0.08	0.06	0.01	0.03	0.04	0.10	0.00
MgO	0.00	0.00	0.00	0.00	0.01	0.00	0.01	0.00	0.00	0.00	0.00	0.00	0.00	0.01	0.01
CaO	6.47	6.43	6.57	6.32	5.91	6.76	6.97	7.00	6.57	6.41	7.06	6.99	6.72	6.93	6.53
Na_2O	6.81	7.04	7.01	7.19	7.58	6.87	6.90	7.12	6.98	7.07	6.44	6.93	6.88	6.87	6.88
K_2O	0.08	0.07	0.05	0.07	0.05	0.06	0.06	0.10	0.10	0.08	0.09	0.06	0.07	0.06	0.09
Total	99.69	99.76	99.58	99.29	99.44	100.14	97.50	99.99	99.56	99.66	98.91	99.68	99.02	99.59	98.68

柏杂岩北界剪切带的涡度与晓天—磨子潭剪切带的涡度值比较吻合,都是简单剪切为主的变形。

(3) 经过矿物动态重结晶的半定量估计以及各地质温压计的定量计算,得出桐柏杂岩北界剪切带的形成条件为压力 $P=0.6\sim0.9$GPa,平均压力约为 0.75GPa,形成温度为 $t=560\sim684$℃,属于高角闪岩相范畴,处于中地壳流变层。李加好等(2011)通过石英和长石的动态重结晶得出商丹断裂带岩石变形温度主要集中在 400 ~ 500℃,故认为商丹断裂带的变形环境介于中—高绿片岩相到低角闪岩相之间。向必伟等(2007)在晓天—磨子潭断裂带中的糜棱岩中得出矿物变形温度在 600 ~ 650℃,利用多硅白云母 + 钾长石 + 石英 + 水组合压力计,获得了 $P=0.99\sim1.17$GPa 的压力值,属于高角闪岩相剪切带。黄鹏等(2015)得出晓天—磨子潭剪切带的变形条件为 $t=599\sim629$℃,平均 618.2℃,压力约 0.7GPa。从而得知,商丹断裂带的变质变形条件要低于桐柏杂岩北界剪切带,而晓天—磨子潭剪切带比较吻合。

(4) 根据中华人民共和国秦岭—大巴山及邻区地质图❶可以发现,桐柏杂岩北界剪切带位于新元古代震旦纪—寒武纪以及泥盆纪南界,晓天—磨子潭剪切带位于新元古代卢镇关群南界和泥盆纪佛子岭群。因此,桐柏杂岩北界剪切带与晓天—磨子潭的北侧都是泥盆纪地层以及新元古代地层,并且,桐柏杂岩北界剪切带和晓天—磨子潭剪切带南缘都是老的变质基底,如果桐柏杂岩北界剪切带沿着泥盆纪南部界线或者变质基底的北部界线延伸则可以延伸到晓天—磨子潭剪切带。所以,从这也可以看出来,桐柏杂岩北界剪切带对应晓天—磨子潭剪切带的西延部分。

(5) 此次通过桐柏杂岩北界剪切带的糜棱岩中的同构造脉体的 U-Pb 锆石定年发现,剪切带的形成以及活动时间为 171 ~ 142 Ma,主要发生在中侏罗世到早白垩世(另文详述)。王勇生等(2009)利用 ^{40}Ar—^{30}Ar 方法得出晓天—磨子潭韧性剪切带的

表 5 桐柏造山带新元古界桐柏杂岩北界剪切带中糜棱岩中黑云母的探针数据以及 Ti—Ms 温度计计算结果

Table 5 The probe data of biotite and the calculation result of Ti—Bt thermometer in the shear zone in northern boundary of the Neoproterozoic Tongbai Complex in the Tongbai orogenic belt

样品(XY-)	t(℃)	P(GPa)	SiO_2	TiO_2	Al_2O_3	FeO^T	MnO	MgO	CaO	Na_2O	K_2O	Si	Ti	Al	Fe	Mg	Na	K	Al^{VI}
30-1	681	0.75	37.41	3.40	14.16	19.92	0.39	8.10	0.34	0.08	8.15	2.95	0.20	1.31	1.31	0.95	0.01	0.82	0.26
30-2	671	0.75	38.25	3.35	14.50	18.28	0.34	9.00	0.59	0.07	7.19	2.97	0.20	1.33	1.19	1.04	0.01	0.71	0.30
30-3	688	0.75	38.23	3.57	14.30	18.12	0.32	8.71	0.67	0.05	6.93	2.99	0.21	1.32	1.18	1.01	0.01	0.69	0.31
30-4	664	0.75	37.47	3.25	14.22	19.69	0.36	8.58	0.50	0.03	7.35	2.95	0.19	1.32	1.30	1.01	0.00	0.74	0.27
30-5	669	0.75	37.79	3.39	14.31	19.93	0.38	8.60	0.26	0.10	8.23	2.94	0.20	1.31	1.30	1.00	0.02	0.82	0.25
31-1	595	0.75	38.52	2.59	14.37	16.14	0.56	11.48	0.07	0.17	9.68	2.95	0.15	1.29	1.03	1.31	0.03	0.94	0.24
31-2	589	0.75	38.79	2.41	14.76	16.10	0.47	11.43	0.05	0.11	9.76	2.95	0.14	1.32	1.02	1.30	0.02	0.95	0.27
31-3	599	0.75	38.59	2.55	14.47	16.46	0.59	10.98	0.08	0.17	9.70	2.95	0.15	1.31	1.05	1.25	0.03	0.95	0.26
31-4	604	0.75	38.18	2.76	14.64	16.28	0.49	11.48	0.09	0.20	9.74	2.92	0.16	1.32	1.04	1.31	0.03	0.95	0.23
31-5	602	0.75	39.06	2.61	14.41	16.37	0.56	11.13	0.07	0.21	9.81	2.97	0.15	1.29	1.04	1.26	0.03	0.95	0.26
33-1	596	0.75	38.55	2.43	14.96	16.55	0.34	10.91	0.10	0.26	9.44	2.95	0.14	1.35	1.06	1.24	0.04	0.92	0.29
33-2	553	0.75	38.54	1.87	14.87	16.66	0.39	11.40	0.07	0.21	9.50	2.95	0.11	1.34	1.07	1.30	0.03	0.93	0.29
33-3	570	0.75	37.34	2.16	14.93	17.11	0.47	11.17	0.06	0.24	9.59	2.89	0.13	1.36	1.11	1.29	0.04	0.95	0.25
33-4	594	0.75	38.19	2.47	14.81	17.05	0.38	10.87	0.05	0.24	9.73	2.93	0.14	1.34	1.09	1.24	0.04	0.95	0.26
33-5	594	0.75	38.09	2.52	15.04	17.24	0.44	11.03	0.04	0.19	9.74	2.90	0.14	1.35	1.10	1.25	0.03	0.95	0.26
35-1	643	0.75	37.54	3.27	13.87	20.16	0.43	9.21	0.00	0.14	9.61	2.91	0.19	1.27	1.31	1.07	0.02	0.95	0.18
35-2	633	0.75	37.82	3.17	13.88	20.52	0.43	9.38	0.01	0.15	9.88	2.91	0.18	1.26	1.32	1.08	0.02	0.97	0.17
35-3	634	0.75	37.85	3.24	13.85	20.68	0.43	9.47	0.00	0.15	9.50	2.91	0.19	1.26	1.33	1.09	0.02	0.93	0.17
35-4	625	0.75	37.44	3.09	13.65	20.55	0.42	9.48	0.00	0.12	9.77	2.91	0.18	1.25	1.33	1.10	0.02	0.97	0.16
35-5	630	0.75	37.69	3.12	13.80	20.38	0.45	9.43	0.00	0.08	9.54	2.92	0.18	1.26	1.32	1.09	0.01	0.94	0.18
37-1	617	0.75	37.31	2.83	14.04	18.00	0.33	10.05	0.06	0.39	8.93	2.93	0.17	1.30	1.18	1.18	0.06	0.89	0.23
37-2	612	0.75	37.73	2.72	14.35	18.06	0.35	10.18	0.00	0.48	8.68	2.93	0.16	1.31	1.17	1.18	0.07	0.86	0.25
37-3	626	0.75	37.31	3.09	14.23	18.68	0.38	10.17	0.01	0.22	8.72	2.90	0.18	1.31	1.22	1.18	0.03	0.87	0.21
37-4	628	0.75	37.65	2.98	14.32	18.18	0.34	10.00	0.02	0.26	8.82	2.93	0.17	1.31	1.18	1.16	0.04	0.88	0.24
37-5	626	0.75	37.31	2.75	15.28	17.88	0.30	9.79	0.02	0.16	8.91	2.90	0.16	1.40	1.16	1.13	0.02	0.88	0.30

形成时间应为 142Ma 之前的晚侏罗世末或早白垩世。而赵淑娟等(2016)研究分析表明在 320 Ma 时,华北陆块和南秦岭微陆块之间的剪刀式拼合导致洛南—栾川剪切带表现为右行剪切,商丹剪切带表现为左行剪切,表示商丹断裂的形成在 320Ma 之前。

通过以上几个方面的对比可以发现,桐柏杂岩北界剪切带的变质变形特征以及活动时间都与晓天—磨子潭剪切带吻合,与商丹断裂带差别较大。故而认为桐柏杂岩北界剪切带对应晓天—磨子潭剪切带的西延部分。

5 结论

(1)通过对桐柏杂岩北界剪切带的观察分析得知,桐柏杂岩北界剪切带是一条大型的左旋平移的韧性剪切带,并且该剪切带内多发育杆状构造,且杆状构造具有层状结构,层与层之间通过一种特殊的滑脱面结合。

(2)桐柏杂岩北界剪切带的有限应变测量值 R_{xz} 在 1.80 ~ 2.04 之间,平均值为 1.95,涡度值 W_k 在 0.82 ~ 0.90 之间,平均值为 0.86,均大于 0.75,说明桐柏杂岩北界剪切带是一条以简单剪切为主,纯剪切为辅的韧性剪切带,反映出此剪切带不是单纯的造山带挤压形成,还受到平行于造山带方向的力的作用,可能与造山带碰撞后的折返机制有关系。

(3)通过角闪石—斜长石—石英温度计、角闪石全 Al 压力计和黑云母中 Ti 温度计可以得知桐柏杂岩北界剪切带的形成条件约为 $t = 560 \sim 684$℃,$P = 0.6 \sim 0.9$GPa,属于高角闪岩相,处于中地壳流变层位置。

(4)通过与商丹断裂带以及晓天—磨子潭剪切带的运动学方向、有限应变及涡度、变质条件以及年代学和地层界线对比可以知道,桐柏杂岩北界剪切带对应晓天—磨子潭剪切带的西延部分,而不是对应商丹断裂带。

注 释 / Note

❶陕西省地质矿产局区域地质调查队. 1992. 中华人民共和国 1:100 万地质图·秦岭—大巴山幅. 地质出版社.

参 考 文 献 / References

(The literature whose publishing year followed by a "&" is in Chinese with English abstract; the literature whose publishing year followed by a "#" is in Chinese without English abstract)

崔建军,胡健民,刘晓春. 2009. 桐柏地区高压变质地体在地壳中的抬升机制. 岩石学报,25(09):2165 ~ 2176.

董云鹏,张国伟,姚安平,赵霞. 2003. 襄樊—广济断裂西段三里岗—三阳构造混杂岩带构造变形与演化. 地质科学,38(04):425 ~ 436.

韩建军,宋传中,李加好,刘欢. 2014. 桐柏—大别南缘殷店—马垅韧性剪切带的变形及年代学分析. 地质科学,49(04):1035 ~ 1044.

黄 鹏,宋传中,任升莲等. 2015. 晓天—磨子潭断裂带构造变形分析及其对大别山构造变形的启示. 地质论评,61(3):512 ~ 524.

黄少英,徐备,王长秋,湛胜,邓荣敬. 2006. 桐柏造山带几何学、运动学和演化. 中国科学,36(3):242 ~ 251.

李炳华. 2001. 秦岭—桐柏—大别造山带深部构造及其与南北两侧陆块关系之探讨. 陕西地质,19(1):59 ~ 70.

李加好,宋传中,任升莲,涂文传,张欢,张浩然. 2010. 秦岭商丹断裂带的构造样式与变形分析. 地学前缘,17(04):197 ~ 205.

李三忠,赵淑娟,李玺瑶,曹花花,刘鑫,郭晓玉,肖文交,赖绍聪,闫臻,李宗会,于胜尧,兰浩圆. 2016a. 东亚原特提斯洋:南北边界和俯冲极性. 岩石学报,32(9):2609 ~ 2627.

李三忠,赵淑娟,余珊,曹花花,李玺瑶,刘鑫,郭晓玉,肖文交,赖绍聪,闫臻,李宗会,于胜尧,张剑,兰浩圆. 2016b. 东亚原特提斯洋:早古生代微陆块亲缘性与聚合. 岩石学报,32(9):2628 ~ 2644.

刘欢,宋传中,林寿发,李加好,黄鹏,王微,杨帆. 2014. 桐柏山 L 构造岩的构造特征与形成环境探讨. 地质科学,49(02):542 ~ 555.

刘欢,林寿发,宋传中. 2016. 桐柏山 L 构造岩形成机制构造解析及其对造山带演化的制约. 地质学报,90(6):1098 ~ 1111.

刘鑫,李三忠,索艳慧,刘晓春,刘恩山,戴黎明. 2010. 桐柏碰撞造山带及其邻区变形特征与构造格局. 岩石学报,26(04):1289 ~ 1302.

刘晓春,江博明,李三忠,崔建军,刘鑫,娄玉行,曲玮. 2011. 桐柏高压变质地体:对桐柏—大别—苏鲁高压/超高压变质带构造框架和俯冲/折返机制的制约. 岩石学报,27(04):1151 ~ 1162.

刘晓春,江博明,李三忠. 2013. 大陆岩板俯冲与折返的穿时性:桐柏造山带晚二叠—三叠纪高压变质地体提供的制约. 科学通报,(23):2251 ~ 2258.

任升莲,宋传中,林寿发,张浩然,李加好,涂文传,章骏杰. 2011. 桐柏山商丹断裂带东延段石榴云母片岩中石榴子石显微构造特征及变质—变形环境分析. 地质论评,57(06):799 ~ 809.

宋传中. 2000. 秦岭—大别山北部后造山期构造格架与形成机制. 合肥工业大学学报(自然科学版),23(02):221 ~ 226.

宋传中,张国伟,任升莲,李加好,黄文成. 2009. 秦岭—大别造山带中几条重要构造带的特征及其意义. 西北大学学报(自然科学版),39(03):368 ~ 380.

索书田,钟增球,游振东. 2001. 大别—苏鲁超高压—高压变质带伸展构造格架及其动力学意义. 地质学报,75(01):14 ~ 24.

索书田,钟增球,张宏飞,周汉文,游振东. 2001. 桐柏山高压变质带及其区域构造型式. 地球科学(中国地质大学学报),26(06):551 ~ 559.

涂文传,宋传中,任升莲,李加好,张欢,张妍,王中. 2012. 秦岭商丹断裂带的构造变形与形成环境分析. 合肥工业大学学报(自然科学版),35(06):820 ~ 827.

王国灿,桑隆康. 1996. 桐柏造山带东段结晶基底杂岩中的大型 A 型背形及其构造背景. 地球科学(中国地质大学学报),21(03):291 ~ 294.

汪洋. 2014. 钙碱性火成岩的角闪石全铝压力计——回顾、评价和应用实例. 地质论评,60(04):839 ~ 850.

王勇生,朱光,向必伟,魏鑫. 2008. 晓天—磨子潭断裂的运动学涡度、应变速率及其大地构造意义. 地学前缘,15(05):376 ~ 387.

王勇生,向必伟,朱光,陈文,魏鑫. 2009. 晓天—磨子潭断裂后造山伸展活动的^{40}Ar-^{39}Ar 年代学记录. 地球化学,38(05):458 ~ 471.

向必伟,朱光,王勇生,谢成龙,胡召齐. 2007. 糜棱岩化过程中矿物变形温度计. 地球科学进展,22(02):126 ~ 135.

徐备,黄少英,湛胜,邓荣敬,刘兵. 2007. 试论桐柏造山带与西大别造山带的对比. 地质学报, 81(1):32 ~ 37.

许光,王二七. 2010. 桐柏杂岩的中生代隆升机制及其与南阳盆地沉降的耦合关系. 地质科学,45(03):626 ~ 652.

杨志坚. 1982. 试论桐柏—大别山地质构造演化特征. 地质学报, 56(2):123 ~ 135.

游振东,钟增球,张泽明. 1999. 桐柏—大别山区高压变质相的构造配置. 地学前缘,6(04):237 ~ 245.

张本仁. 2005. 地球化学进展:化学工业出版社.

张国伟,孟庆任,于在平,孙勇,周鼎武,郭安林. 1996. 秦岭造山带的造山过程及其动力学特征. 中国科学,26(3):193 ~ 200.

张国伟,柳小明. 1998. 关于"中央造山带"几个问题的思考. 地球科学(中国地质大学学报),23(05):443 ~ 448.

张国伟. 2001. 秦岭造山带与大陆动力学:科学出版社.

张宏飞,张利,高山,张本仁,王林森. 1999. 桐柏地区变质杂岩和侵入岩类 Pb 同位素组成特征及其地质意义. 地球科学,24(03):269 ~ 273.

赵淑娟,李三忠,余珊,李玺瑶,曹花花,刘鑫,王鹏程. 2016. 东亚原特提斯洋:北秦岭韧性剪切带构造特征. 岩石学报,32(9):2645 ~ 2655.

郑亚东,王涛,张进江. 2008. 运动学涡度的理论与实践. 地学前缘,15(03):209 ~ 220.

钟增球,索书田,张宏飞,周汉文. 2001. 桐柏—大别碰撞造山带的基本组成与结构. 地球科学,26(06):560 ~ 567.

Anderson D J, Lindaley D H, Dabidson P M. 1993. ILF: A Pascal program to assess equilibria among Fe—Mg—Mn—Ti oxides, pyroxenes, olivine and quartz. Computers and Geosciences, 19: 1333 ~ 350.

Anderson J L, Smith D R. 2015. The effects of temperature and fO_2 on the Al-in-hornblende barometer. American Mineralogist, 80(5 ~ 6): 549 ~ 559.

Cates A E, Clover L. 1989. Alleghanian tectono—thernal evolution of the dextral transcurrent hylas zone, Virginia Piedmont, USA. Journal of Structure Geology, 11: 407 ~ 419.

Cui Jianjun, Hu Jianmin, Liu Xxiaochun. 2009&. Exhumation of high-pressure metamourphic terrane at the crustal levels in the Tongbai area, central China. Acta Petrologica Sinica, 25(09): 2165 ~ 2176.

Daalen M V, Heilbronner R, Kunze K. 1999. Orientation analysis of localized shear deformation in quartz fibres at the brittle - ductile transition. Tectonophysics, 303(1 ~ 4): 83 ~ 107.

Dong Yunpeng, Zhang Guowei, Yao Anping, Zhao Xxia. 2003&. Deformation and evolution of the Sanligang—Sanyang tectonic mélange belt along the west sector of Xiangfan—Guangji fault. Chinese Journal of Geology, 38(04): 425 ~ 436.

Eide E A, Mcwilliams M O, Liou J G. 1994. ^{40}Ar/^{39}Ar geochronology and exhumation of high-pressure to ultrahigh-pressure metamorphic rocks in east—central China. Geology, 22(7): 601 ~ 604.

Ernst W G, Tsujimori T, Zhang R, Liou J G. 2007. Permo-Triassic Collision, Subduction-Zone Metamorphism, and Tectonic Exhumation Along the East Asian Continental Margin. Annual Review of Earth & Planetary Sciences, 35(1): 73 ~ 110.

Faure M, Lin W, Shu L, Sun Y, Schärer U. 1999. Tectonics of the Dabieshan (eastern China) and possible exhumation mechanism of ultrahigh-pressure rocks. Terra Nova, 11(11): 251 ~ 258.

Faure M, Lin W, Monié P, Breton N L, Poussineau S, Panis D, Deloule E. 2003. Exhumation tectonics of the ultrahigh-pressure metamorphic rocks in the Qinling orogen in east China: New petrological—structural—radiometric insights from the Shandong Peninsula. Tectonics, 22(3): 127 ~ 143.

Hacker B R. 1995. What brought them up? Exhuming the Dabie Shan ultrahigh-pressure rocks. Geology, 23(8): 743.

Hacker B R, Ratschbacher L, Webb L, Mcwilliams M O, Ireland T, Calvert A, Chateigner D. 2000. Exhumation of ultrahigh-pressure continental crust in east central China: Late Triassic—Early Jurassic tectonic unroofing. Journal of Geophysical Research Solid Earth, 105(B6): 13339 ~ 13364.

Hammarstrom J M, Zen E A. 1986. Aluminum in hornblende: An empirical igneousgeobarometer. American Mineralogist, 71(11): 1297 ~ 1313.

Han Jianjun, Song Chuanzhong, Li Jiahao, Liu Huan. 2014&. Deformation analysis and chronological dating of Yindian—Malong ductile shear zone in the southern margin of Tongbai—Dabie orogenic belt. Chinese Journal of Geology, 49(04): 1035 ~ 1044.

Holland T J B, Blundy J D. 1994. Non-ideal interactions in calcic amphiboles and their bearing on amphibole—plagioclase thermometry. Contributions to Mineralogy and Petrology, 116: 433 ~ 447.

Hollister L S, Grissom G C, Peters E K, Stowell H H, Sisson V B. 1987. Confirmation of the empirical correlation of A1 in hornblende with pressure of solidification of calc-alkaline plutons. Am. Mineral. American Mineralogist, 72(3): 231 ~ 239.

Huang Peng, Song Chuanzhong, Ren Shenglian, Lin Shoufa, Zhang Yan, Li Jiahao, Gong Long, Liu Huan, Wang Wei. 2015&. Analysis on structural deformation of Xiaotian—Mozitan shear zone and it's implication on Dabie orogen. Geological Review, 61(3): 512 ~ 524.

Huang Shaoying, Xu Bei, Wang Changqiu, Zhan Sheng and Deng Rongjing. 2006&. The geometry, kinematics and evolution of the Tongbai orogenic belt. Science in China, 36(3): 242 ~ 251.

Johnson M C and Rutherford M J. 1988. Experimental calibration of an aluminum-in-hornblende geobarometer applicable to calcic-alkaline rocks. EOS, 69: 1511.

Johnson M C, Rutherford M J. 1989. Experimental calibration of the aluminum-in-hornblende geobaromrter with application to Long Valley caldera(Califomia). Geology, 17: 837 ~ 841.

Lafrance B, John E, Frost B R. 1998. Ultrahigh-temperature and subsolidus shear zones: example from the Poe Moutain anorthosite, Wyoming. Journal of Structure Geology, 945 ~ 955.

Li Binghua. 2001&. Discussion on the deep-seated structures of the Qinling—Tongbai—Dabieshan orogenic belt and its relations with the landmass on its south and north sides. Geology of Shanxi, 19(1): 59 ~ 70.

Li Jiahao, Song Chuanzhong, Ren Shenglian, Tu Wenchuan, Zhang Huan, Zhang Haoran. 2010&. Tectonic style and deformation analysis of Shangdan fault belt in Qinling Orogen. Earth Science Frontiers, 17(4): 197 ~ 205.

Li S Z, Kusky T M, Wang L, Zhang G, Lai S, Liu X, Zhao G. 2007. Collision leading to multiple-stage large-scale extrusion in the Qinling orogen: Insights from the Mianlue suture. Gondwana Research, 12(1): 121 ~ 143.

Li S Z, Kusky T M, Liu X, Zhang G, Zhao G, Wang L, Wang Y. 2009. Two-stage collision-related extrusion of the western Dabie HP - UHP metamorphic terranes, central China: Evidence from quartz c - axis fabrics and structures. Gondwana Research, 16(2): 294 ~ 309.

Li S Z, Kusky T M, Zhao G, Liu X, Zhang G, Kopp H, Wang L. 2010. Two-stage Triassic exhumation of HP—UHP terranes in the western Dabie orogen of China: Constraints from structural geology. Tectonophysics, 490(3): 267 ~ 293.

Li Sanzhong, Zhao Shujuan, Li Xiyao, Cao Huahua, Liu Xin, Guo Xiaoyu, Xiao Wenjiao, Lai Shaocong, Yan Zhen, Li Zonghui, Yu Shengyao and Lan Haoyuan. 2016a&. Proto-Tehtys Ocean in East Asia: Northern and southern border faults and subduction polarity. Acta Petrologica Sinica, 32(9): 2609 ~ 2627.

Li Sanzhong, Zhao Shujuan, Yu Shan, Cao Huahua, Li Xiyao, Liu Xin, Guo Xiaoyu, Xiao Wenjiao, Lai Shaocong, Yan Zhen, Li Zonghui, Yu Shengyao, Zhang Jian and Lan Haoyuan. 2016b&. Proto-Tehtys Ocean in East Asia: Affinity and assembly of Early Paleozoic micro-continental blocks. Acta Petrologica Sinica, 32(9): 2628 ~ 2644.

Lin Wei, Shi Yonghong, Wang Qingchen. 2009. Exhumation tectonics of the HP—UHP orogenic belt in Eastern China: New structural - petrological insights from the Tongcheng massif, Eastern Dabieshan. Lithos, 109(3 ~ 4): 285 ~ 303.

Liu Huan, Song Chuanzhong, Lin Shoufa, Li Jiahao, Huang Peng, Wang Wei and Yang Fan. 2014&. Study on structural features and *P—T* conditions of the L tectonites in the Tongbai mountains. Chinese Journal of Geology, 49(02): 542 ~ 555.

Liu Huan, Lin Shoufa, Song Chuanzhong. 2016&. The structure formation mechanism of L tectonites in Tongbai mountain and its constraints on the orogenic evolution. Acta Geologica Sinica, 90(6): 1098 ~ 1111.

Liu Xin, Li Sanzhong, Suo Huiyan, Liu Xiaochun, Liu Enshan and Dai Liming. 2010&. Tectonic outline and structural styles of the Tongbai collisional orogeny and its neighbors. Acta Petrologica Sinica, 26(04): 1289 ~ 1302.

Liu Xiaochun, Lou Yuxing, Dong Shuwen. 2005. *P—T* path of low-temperature eclogites from the Tongbaishan area. Acta Petrologica Sinica, 21(4): 1081 ~ 1093.

Liu Xiaochun, Jahn B M, Dong Shuwen, Lou Yuxing, Cui Jianjun. 2008. High-pressure metamorphic rocks from Tongbaishan, central China: U-Pb and $^{40}Ar/^{39}Ar$ age constraints on the provenance of protoliths and timing of metamorphism. Lithos, 105(3 ~ 4): 301 ~ 318.

Liu Xiaochun, Jahn B M, Li Sanzhong, Cui Jianjun, Liu Xin, Lou Yuxing and Qu Wei. 2011&. The Tongbai HP metamorphic terrane: Constraintson the architecture and subduction/exhumation of the Tongbai—Dabie—Sulu HP/UHP metamorphic belt. Acta Petrologica Sinica, 27(4): 1151 ~ 1162.

Liu Xiaochun, Jiang B M, Li Sanzhong. 2013&. Subduction and exhumation of rock plate, diachroneity: restricting Tongbai orogenic belt two late Triassic UHP metamorphic terrane provided. Chinese Science Bulletin, (23): 2251 ~ 2258.

Lv B, Zhai M, Li T, Peng P. 2013. Ziron U-Pb ages and geochemistry of the Qinglong volcano-sedimentary rock series in Eastern Hebei: Implication for 2500 Ma intracontinental rifting in the North China Craton. Paper presented at the Institute of Geology and Geophysics.

Okay A I, Celal A M, Satir M. 1993. Tectonics of an ultrahigh-pressure metamorphic terrane: The Dabie Shan/Tongbai Shan Orogen, China. Tectonics, 12(6): 1320 ~ 1334.

Pryer L L. 1993. Microstructures in feldspars from a major crustal thrust zone, the Grenville Front, Ontario, Canada. Journal of Structure Geology, 15: 21 ~ 36.

Ratschbacher L, Hacker B R, Webb L E, Mcwilliams M, Ireland T, Dong S, Wenk H R. 2000. Exhumation of the ultrahigh-pressure continental crust in east central China: Cretaceous and Cenozoic unroofing and the Tan-Lu fault. Journal of Geophysical Research Solid Earth, 105(B6): 13303 ~ 13338.

Ren Shenglian, Song Chuanzhong, Lin Shoufa, Zhang Haoran, Li Jiahao, Tu Wenchuan and Zhang Junjie. 2011&. The study of microstructure characters and the condition of metamorphism and deformation of garnets from garnet—mica schist in the Tongbai Moutain, east section of Shangnan—Danfeng fault belt. Geological Review, 57(06): 799 ~ 809.

Schmidt M W. 1992. Amphibole composition in tonalite as a function of pressur: an experimental calibration of the Al-in-hornblende barometer. Contributions to Mineralogy & Petrology, 110(2 ~ 3): 304 ~ 310.

Simpson C. 1985. Deformation of granitic rocks across the brittle—ductile transition. Journal of Structure Geology, 7: 503 ~ 511.

Song Chuanzhong. 2000&. Late orogenic tectonics and forming mechanism in the north of Qinling—Dabie mountains. Journal of Heifei University of Technology, 23(02): 221 ~ 226.

Song Chuanzhong, Zhang Guowei, Ren Shenglian, Li Jiahao and Hunag Wencheng. 2009&. The research on deformation features of some structural zones in the Qinling—Dabieshan orogenic belt. Journal of Northwestern University, 36(3): 242 ~ 251.

Suo Shutian, Zhong Zengqiu, You Zhendong. 2001&. Extension tectonic framework of the Dabie—Sulu UHP—HP metamorphic belt, central China, and its geodynamical significance. Acta Geologica Sinica, 75(01): 14 ~ 24.

Suo Shutian, Zhong Zengqiu, Zhang Hongfei, Zhou Hanwen and You Zhendong. 2001&. High-pressure metamorphic belt and its tectonic pattern in Tongbai mountains, central China. Earth Science——Journal of China University of Geosciences, 26(06): 551 ~ 559.

Tikoff B, Fossen H. 1995. The limitations of three-dimensional kinematic vorticity analysis. Journal of Structural Geology, 17(12): 1771 ~ 1784.

Tu Wenchuan, Song Chuanzhong, Ren Shenglian, Li Jiahao, Zhang Huan and Zhang Yan, Wang Zhong. 2012&. An analysis of tectonic deformation and forming environment of Shangdan fault zone, Qinling. Journal of Heifei University of Technology, 35(06): 820 ~ 827.

Wang E, Meng Q, Burchfiel B C, Zhang G. 2003. Mesozoic large-scale lateral extrusion, rotation, and uplift of the Tongbai Dabie Shan belt in east China. Geology, 31(4): 307 ~ 310.

Wang Gguochan, Sang Longkang. 1996&. A gigantic a-type antiform and its tectonic setting in Tongbai gneiss complex, eastern Tongbai orogen, central China. Earth Science——Journal of China University of Geosciences, 21(03): 291 ~ 294.

Wang Yang. 2014&. The Al-in-hornblende barometry for Calc-alkaaline igneous rocks: retrospect, evaluation and applications. Geological Review, 60(04): 839 ~ 850.

Wang Yongsheng, Zhu Guang, Xiang Biwei, Wei Xin. 2008&. The kinematic vorticity and strain rate of Xiaotian—Mozitan fault and their tectonic significance. Earth Science Frontiers, 15(5): 376 ~ 387.

Wang Yongsheng, Xiang Biwei, Zhu Guang, Chen Wen and Wei Xin. 2009&. ^{40}Ar-^{39}Ar Geochronology records for post-orogenic extension of the Xiaotian—Mozitan fault. Geochimica, 38(05): 458 ~ 471.

Webb L E, Hacker B R, Ratschbacher L, Mcwilliams M O, Dong S. 1999. Thermochronologic constraints on deformation and cooling history of high and ultrahigh-pressure rocks in the Qinling—Dabie orogen, eastern China. Tectonics, 18(4): 621 ~ 638.

Webb L E, Ratschbacher L, Hacker B R, Dong S. 2001. Kinematics of exhumation of high- and ultrahigh-pressure rocks in the Hongân and Tongbai Shan of the Qinling—Dabie collisional orogen, eastern China. Memoir of the Geological Society of America, 194: 231 ~ 245.

Wu Chunming, Chen Haixia. 2015. Revised Ti-in-biotite geothermometer for ilmenite- or rutile-bearing crustal metapelites. Science Bulletin, 60(1): 116 ~ 121.

Wu Y B, Gao S, Zhang H F, Yang S H, Jiao W F, Liu Y S, Yuan H L. 2008. Timing of UHP metamorphism in the Hong'an area, western Dabie Mountains, China: evidence from zircon U-Pb age, trace element and Hf isotope composition. Contributions to Mineralogy & Petrology, 155(1): 123 ~ 133.

Xiang Biwei, Zhu Guang, Wang Yongsheng, Xie Chenglong and Hu Zhaoqi. 2007&. Mineral deformation thermometer for mylonitization. Advances in Earth Science, 22(02): 126 ~ 135.

Xu Bei, Huang Shaoying, Zhan Sheng, Deng Rongjing, Liu Bing. 2007&. Correlation between Tongbai and Western Dabie orogenic belts. Acta Geologica Sinica, 81(1): 32 ~ 37.

Xu Guang, Wang Erqi. 2010&. The uplift mechanism of Tongbai complex in Mesozoic and its coupling relationship with Nanyang Basin. Chinese Journal of Geology, 45(03): 626 ~ 652.

Xu Z Q, Zeng L S, Liu F L, Yang J S, Zhang Z M, Mcwilliams M O, Liou J G. 2006. Polyphase subduction and exhumation of the Sulu high-pressure—ultrahigh-pressure metamorphic terrane. Special Paper of the Geological Society of America, 403(1): 324 ~ 328.

Yang Zhijian. 1982&. The characteristics of the geological and tectonic evolution of the Tongbai – Dabie Mountains. Acta Geologica Sinica, 81(1): 32 ~ 37.

You Zhendong, Zhong Zengqiu, Zhang Zeming. 1999&. The Tectonic distribution of high-pressure metamorphic facies in Tongbai—Dabieshan, central China. Earth Science Frontiers, 6(04): 237 ~ 245.

Zhang Benren. 2005&. Advances in geochemistry: Chemical Industry Press.

Zhang Guowei, Meng Qqingren, Yu Zaiping, Sun Yong, Zhou Dingwu and Guo Anlin. 1996&. The orogenic process and dynamic characteristics of the Qinling Mountains orogenic belt. Science in China, 26(3): 193 ~ 200.

Zhang Guowei, Liu Xiaoming. 1998&. Some remarks on China central orogenic system. Earth Science, 23(05): 443 ~ 448.

Zhang Guowei. 2001&. Qinling mountains orogenic belt and continental dynamics. Beijing: Science Press.

Zhang H, Zhong Z, Gao S, Zhang B, Zhang L, Hu S, Hou Q. 2004. Pb and Nd isotopic composition of the Jigongshan granite: constraints on crustal structure of Tongbaishan in the middle part of the Qinling—Tongbai—Dabie orogenic belt, Central China. Lithos, 73(3 ~ 4): 215 ~ 227.

Zhang Hongfei, Zhang Li, Gao Shan, Zhang Benren and Wang Linsen. 1999&. Pb isotopic compsitions of metamorphic rocks and intrusive rocks in Tongbai region and their geological implication. Earth Science, 24(03): 269 ~ 273.

Zhang R Y, Liou J G. 1994. Significance of magnesite paragenesis in ultrahigh-pressure metamorphic rocks. American Mineralogist, 79(3 ~ 4): 397 ~ 400.

Zhao Shujuan, Li Sanzhong, Yu Shan, Li Xiyao, Cao Huahua, Liu Xin, Wang Pengcheng. 2016&. Proto-Tehtys Ocean in East Asia: Structures of ductile shear zones in the North Qinling. Acta Petrologica Sinica, 32(9): 2645 ~ 2655.

Zheng Yadong, Wang Tao, Zhang Jinjiang. 2008&. Theory and practice of kinematic vorticity. Earth Science Frontiers, 15(03): 209 ~ 220.

Zheng Y F, Fu B, Gong B, Li L. 2003. Stable isotope geochemistry of ultrahigh pressure metamorphic rocks from the Dabie—Sulu orogen in China: implications for geodynamics and fluid regime. Earth Science Reviews, 62(1 ~ 2): 105 ~ 161.

Zheng Y F, Gao T S, Wu Y B, Gong B, Liu X M. 2007. Fluid flow during exhumation of deeply subducted continental crust: zircon U-Pb age and O-isotope studies of a quartz vein within ultrahigh-pressure eclogite. Journal of Metamorphic Geology, 25(2): 267 ~ 283.

Zhong Zengqiu, Suo Shutian, Zhang Hongfei, Zhou Hanwen. 2001&. Major constitutes and texture of the Tongbai—Dabie collisional orogenic belt. Earth Science, 26(06): 560 ~ 567.

Zhou J B, Wilde S A, Zhao G C, Zheng C Q, Jin W, Zhang X Z, Cheng H. 2008. Detrital zircon U-Pb dating of low-grade metamorphic rocks in the Sulu UHP belt: Evidence for over thrusting of the North China Craton onto the South China Craton during continental subduction. Journal of the Geological Society, 165(9): 423 ~ 433.

Metamorphism and Deformation Analysis of the Shear Zone in the Northern Boundary of the Tongbai Complex and Discussion on Its Ascription

LI Hailong, SONG Chuanzhong, LI Jiahao, REN Shenglian, ZHANG Yan, WANG Wei, YANG Fan

School of Resources and Environmental Engineering, Hefei University of Technology, Hefei, 230009

Objectives: The Qinling—Tongbai—Dabie collision orogenic belt is the largest high-ultrahigh pressure structural zone in the world. There are two large ductile shear zones on both sides of the orogenic belt, and geological scholars have done more study on the Yindian—Malong shear zone in the south of Tongbai complex. But there is few study on the shear zone in the north of Tongbai complex. This project uses a variety of methods to study and cognize the large ductile shear zone intensively, but also discusses its ascription.

Methods: On the basis of detailed field observation, we combine the analysis of indoor microstructure analysis, finite strain measurement, vorticity calculation, dynamic recrystallization of quartz and feldspar, hornblende total Al pressure gauge, hornblende—plagioclase—quartz thermometer and single mineral thermometer of biotite to study the

shear zone in northern boundary of Tongbai complex. And according to these features of the shear zone, we make comparative analysis with the Shangdan fault in the west and the Xiaotian—Mozitan shear zone in the east to limit the ascription of the shear zone in northern boundary of Tongbai complex.

Results: Through our observation and analysis, we found that the shear zone in northern boundary of Tongbai Complex is a sinistral ductile shear belt, and the shear zone developed rodding structure with layer structure. There is a special detachment surface binding between layers. Through microscopic analysis and measurement we know that the finite strain measurement value R_{xz} is between 1.80 ~ 2.04, and the average is 1.95, the vorticity value W_k is between 0.82 ~ 0.90, the average is 0.86, which is greater than 0.75 and indicates that the shear zone in northern boundary of Tongbai Complex is mainly simple sheared, supplemented by pure shearing. Through the dynamic recrystallization of quartz and feldspar and hornblende total Al pressure gauge, hornblende—plagioclase—quartz thermometer and Ti in biotite thermometer, we know that the formation conditions of the shear zone in northern boundary of Tongbai Complex are about $t = 560 \sim 684$℃, $P = 0.6 \sim 0.9$ GPa, belonging to the high amphibolite facies, which is in a crustal rheological layer position.

Conclusions: Through our detailed field observation and indoor analysis on the shear zone in northern boundary of Tongbai complex, we know that the shear zone is a sinistral ductile shear belt and develops rodding structure with layer structure. The vorticity value indicates that the shear zone in northern boundary of Tongbai Complex is mainly simple sheared, supplemented by pure shearing, reflecting the shear band's formation is not only influenced by extrusion, but also affected by the force paralleled to the orogenic belt, which may be related to the mechanism of reentry after collision of orogenic belt. By the comparison with the Shangdan fault zone and the Xiaotian—Mozitan shear zone we can know that the shear zone in northern boundary of Tongbai Complex belongs to Xiaotian—Mozitan shear zone, rather than the Shangdan fault zone.

Keywords: Tongbai Complex, the ductile shear belt, layer structure, detachment surface, finite strain, vorticity

Acknowledgements: This research was supported by the National Natural Science Foundation of China (No.s: 41272222, 41502193).

First author: LI Hailong, male, born in 1991, a doctoral candidate of Hefei University of Technology and majored in structural geology. Email: sargnlee@126.com

Corresponding author: SONG Chuanzhong, male, born in 1954. a professor of Hefei University of Technology, mainly engaged in the teaching and research of structural geology. Email: czsong69@163.com

Manuscript received on: 2016-09-06; Accepted on: 2017-02-17; Edited by: LIU Zhiqiang.

Doi: 10.16509/j.georeview.2017.02.008